



OPEN

Dynamics of post-occlusion water diffusion in stratum corneum

Ivan Argatov^{1,2}, Felix Roosen-Runge^{2,3} & Vitaly Kocherbitov^{2,3}✉

Diffusion of water through membranes presents a considerable challenge, as the diffusivity often depends on the local concentration of water. One particular example with strong biological relevance is the stratum corneum (SC) as the primary permeability barrier for the skin. A simple alternative for the constant diffusivity model is provided by the Fujita's two-parameter rational approximation, which captures the experimentally observed fact that the SC diffusion constant for water increases with increasing the water concentration. Based on Fick's law of diffusion, a one-dimensional concentration-dependent diffusion model is developed and applied for the analysis of both the steady-state transepidermal water loss (TEWL) and the non-steady-state so-called skin surface water loss (SSWL) occurred after removal of an occlusion patch from the SC surface. It is shown that some of the age-related changes in the SSWL can be qualitatively explained by the variation of the dimensionless Fujita concentration-dependence parameter.

The stratum corneum (SC) is the most outer layer of the skin, which is of paramount importance for maintaining the skin's barrier function integrity. One of the essential functions of the SC is to maintain a healthy level of water loss through the skin, and a detailed understanding of the underlying mechanisms governing the water diffusivity would thus be of high relevance for pharmacy and biomedicine. Typically, the transepidermal water loss (TEWL) as central indicator is evaluated under the conditions of steady state, providing an in vivo assessment of the SC water diffusion. However, this signature misses essential insights into the underlying mechanisms, and should thus be complemented with dynamical methods addressing diffusion outside of the steady state¹.

One possibility for the in vivo dynamical analysis of water diffusion in SC is provided by the so-called plastic occlusion stress test (POST), which modifies the initial hydration conditions in SC for the evaluation of the skin surface water loss (SSWL). It is suggested that by application of an occlusive patch for a few hours, the occluded SC membrane achieves the fully hydrated state. Therefore, following the removal of the occlusion patch, the water-desorption curve represents the temporary variation of SSWL, which gradually decreases towards the baseline value of TEWL, measured at the same level of ambient humidity.

To date, a number of approaches have been put forward for mathematical modeling of the POST-induced SSWL. A simple biexponential fitting analysis of SSWL was first suggested², based on the analysis of the Fickian diffusion with constant diffusivity. A disposition-decomposition analysis based phenomenological approach was developed¹ by incorporating epidermal "capacitance" measurements. A two-compartment model, which simulates the SC membrane and the inner skin layers as two biocompartments with different water diffusivities, was introduced³ to understand the in vivo cutaneous water balance dynamics. Since the diffusion coefficient of water in SC highly depends on the degree of hydration, the effect of a concentration-dependent diffusivity on the relaxation of perturbed TEWL is expected to be significant².

This study is motivated by a clear problem in interpreting experimental evidence based on any model with constant water diffusion coefficient throughout the SC. The SC membrane is known for superior barrier functions, which should be maintained during life in spite of aging. The experimental evidence shows that (I) the TEWL does not change with age, (II) the initial post-occlusion SSWL is found to significantly increase with age² as well as (III) the water content in aged SC is lower than that in young SC⁴. When trying to cope with these facts within the framework of the Fick's law based model with a constant diffusivity, D , we realize that a contradiction arises from combining observations (I) and (II) with other experimental evidence (III) observed for SC. Indeed, it can be shown (see Remark 1 and Section I, SI) that the TEWL and the initial post-occlusion SSWL are respectively proportional to D/δ and \sqrt{D} , where δ denotes the SC thickness, whereas the water content is simply proportional to δ . That is why, from (I) and (II), it follows that both D and δ should increase with age, but condition (III) implies that δ decreases with age. This contradiction shows that the constant diffusivity model does not allow to model the age-related alterations in the SC diffusion properties.

¹Institut für Mechanik, Technische Universität Berlin, 10623 Berlin, Germany. ²Faculty of Health and Society, Malmö University, 205 06 Malmö, Sweden. ³Biofilms-Research Center for Biointerfaces, Malmö University, 205 06 Malmö, Sweden. ✉email: vitaly.kocherbitov@mau.se

A substantial body of experimental evidence reveals the fact that the SC diffusivity is concentration dependent. While clearly more appropriate, a concentration-dependent diffusivity poses essential questions for data interpretation, as the evaluation of experimental signatures becomes in general more complicated. Thus, there is the need to establish a simple but sufficiently flexible functional dependence of the diffusivity D on the water concentration, c . A good candidate for approximating the function $D(c)$ is found to be provided by the two-parameter model $D(c) = D_0/(1 - \lambda c)$ that was suggested by Fujita⁵ for polymers.

In the present study, we apply the Fick's law based classical one-dimensional model to water diffusion in SC with a concentration-dependent diffusivity. In terms of the common classification⁶, this model is a transient basic model, which is non-linear due to the dependency of the SC diffusivity on the concentration of the permeating solute. With the aim of obtaining analytical solutions, we introduce the two-parameter Fujita fitting model for describing the SC water diffusivity. An efficient procedure for evaluating the model parameters from the POST-induced variation of SSWL has been developed.

The rest of the paper is organized as follows. In section "Theory", we develop a one-dimensional diffusion model for a SC membrane based on Fick's laws and Fujita's concentration-dependent approximation for the SC diffusivity, by paying a particular attention to the transepidermal water loss (TEWL), water concentration profile, water content, wet thickness of SC, time lag associated with desorption after application of occlusion, and approximately evaluate in explicit form the skin surface water loss (SSWL) as the desorption water flux from a semi-infinite medium. In section "Results", first, we concretize the main relations for the Fujita approximation-based model and perform its cross-validation by utilizing a data set available in the literature. Then, we apply the developed model for the analysis of post-occlusion SSWL and age-related changes in the SC diffusivity. Finally, we outline a discussion of the obtained results and formulate our conclusions.

Theory

Simple fitting approximation for the SC diffusivity. Several different model functions have been proposed to model the water diffusivity as a function of the water concentration. Based on an analysis of experimental data available in the literature, the following formula has been suggested for the diffusivity, D (cm²/s), of normal human SC⁷:

$$D \times 10^9 = 0.4331 - 0.3765 \exp(-9.6215c) + 0.00006428 \exp(12.873c), \quad (1)$$

which will be referred to as the bi-exponential approximation. Also, based on the analysis performed previously by Stockdale⁸, the following more simple formula has been also suggested⁷:

$$\frac{D}{D_1} = \frac{0.175c_1}{c_1 - c} + 0.46, \quad (2)$$

where $c_1 = 0.835 \text{ g cm}^{-3}$ and $D_1 = 0.6 \times 10^{-9} \text{ cm}^2/\text{s}$.

As it was pointed out⁷, formula (2) predicts a steep rise in water diffusivity D as the water concentration c approaches a limiting value c_1 , which is taken to be greater than c_h , while the latter value was estimated to be 0.78 g cm^{-3} for fully hydrated skin. It is to note here that the second term in formula (1) accounts for a gradual increase in the water diffusivity of dry SC tissue observed in in vitro studies⁹.

As a further simplification over the Stockdale approximation (2), the following two-parameter simple fitting formula has been proposed by Fujita⁵:

$$D = \frac{D_0}{1 - \lambda c}. \quad (3)$$

The parameters $D_0 = 2.07013 \times 10^{-10} \text{ cm}^2/\text{s}$ and $\lambda = 1.13887$ of formula (3) are obtained by fitting to formula (1) in the range $0.2 \leq c \leq 0.78 \text{ g cm}^{-3}$, which covers the common interval of in vivo human skin hydration⁷. The choice of formula (3) was motivated by its utility in describing the growing dependence of the diffusivity D on the concentration c with a reasonable simple functional form which still allows systematic and physical variations.

The variations of the SC diffusivity as predicted by formulas (1), (2), and (3) are shown in Fig. 1a. An undeniable advantage of formula (3), which was earlier introduced by Fujita⁵ for describing the diffusion of low-molecular-weight substances into high-polymeric solids, is that it allows to derive simple analytical estimates for the dynamic diffusion process.

Fick's laws and boundary conditions. To interpret in vivo data on the water diffusion process in stratum corneum (SC), we apply Fick's second and first laws

$$\frac{\partial c}{\partial t} = \frac{\partial}{\partial x} \left(D(c) \frac{\partial c}{\partial x} \right), \quad J = -D(c) \frac{\partial c}{\partial x} \quad (4)$$

with a concentration-dependent diffusivity $D(c)$, where $c = \rho_w \phi_w$ is the water concentration in the SC membrane, ρ_w is the density of water (1 g cm^{-3}), ϕ_w is the water volume fraction, and J is the water flux. The SC diffusivity is usually measured in cm²/s.

For in vivo conditions, we assume that the concentration c varies from c_0 at the free surface, $x = 0$, to the fully hydrated value c_h at a depth where SC merges into the viable tissues (see Fig. 2a)¹⁰. While the value of c_h is a constant (e.g., 0.88 g cm^{-3} , as suggested¹⁰), the value of c_0 depends on the relative humidity of the air. In the steady state conditions, when the concentration c does not vary with time, the boundary conditions take the form

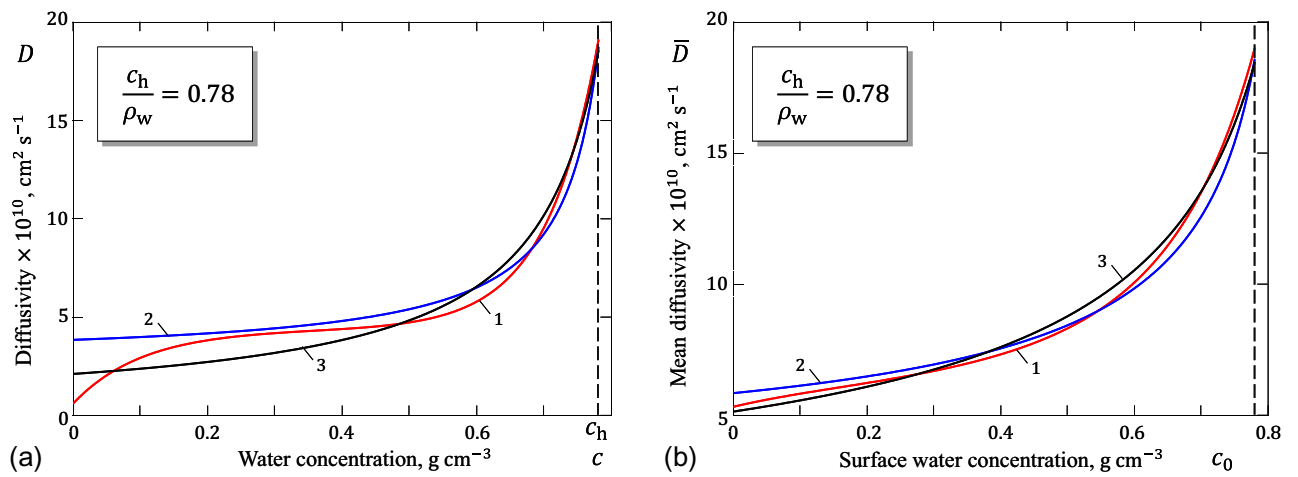


Figure 1. (a) Diffusivity of stratum corneum; (b) Mean diffusivity of stratum corneum. Curves 1, 2, and 3 correspond to formulas (1), (2), and (3), respectively.

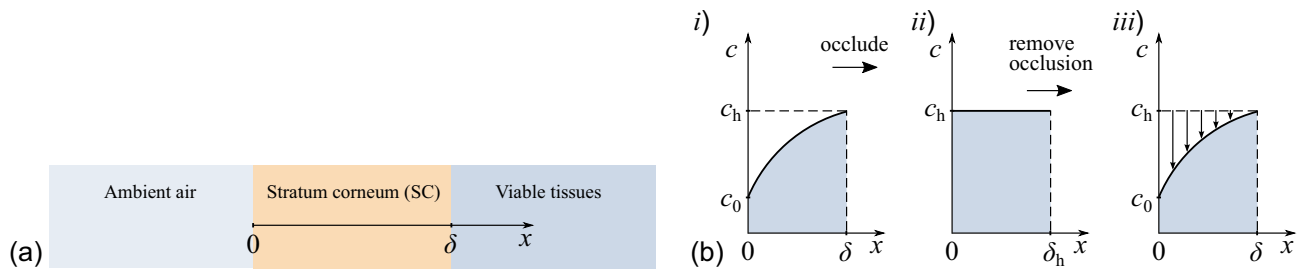


Figure 2. Schematics (a) of a SC membrane and (b) of the occlusion-induced changes in the water concentration profile across the stratum corneum (after²).

$$c|_{x=0} = c_0, \quad c|_{x=\delta} = c_h, \tag{5}$$

where δ is the thickness of SC in vivo.

It is interesting that the SC compartment model¹¹ is based on a discrete variant of Fick’s first law (4)₂.

Transepidermal water loss (TEWL). In the steady state, the left-hand side of Eq. (4)₁ equals zero, and its integration with respect to x leads to Eq. (4)₂ with a constant left-hand side, which will be denoted as $-J_\infty$. In turn, the integration of Eq. (4)₂ yields the following well-known results¹²:

$$J_\infty = \frac{1}{\delta} \int_{c_0}^{c_h} D(u) du = \frac{\bar{D}}{\delta} (c_h - c_0), \quad \bar{D} = \frac{1}{c_h - c_0} \int_{c_0}^{c_h} D(u) du. \tag{6}$$

Here, u denotes the integration variable, and \bar{D} is the mean diffusion coefficient.

The variation of \bar{D} as a function of c_0 is illustrated in Fig. 1b for typical variations of the SC diffusivity. Interestingly, the difference between the diffusivity curves diminishes under the operation of averaging. This, in particular, means that experimental errors may have a strong impact on the diffusivity variation $D(c)$, determined from the measurement of the steady-state water flux, since in such experiments one actually measures the mean diffusivity \bar{D} .

Water concentration profile. The water concentration profile, $c(x)$, is given in the implicit form by the following equation¹⁰:

$$\frac{x}{\delta} = \left(\int_{c_0}^{c_h} D(u) du \right)^{-1} \int_{c_0}^c D(u) du. \tag{7}$$

To determine the value $c(x)$ for a given coordinate x , in the general case, Eq. (7) should be solved numerically.

The variation of the relative water concentration profile $c(x)/c_h$ as a function of the relative in-depth coordinate x/δ is illustrated in Fig. 3a for the typical variations of the SC diffusivity when $c_0/c_h = 0.2$. Observe that

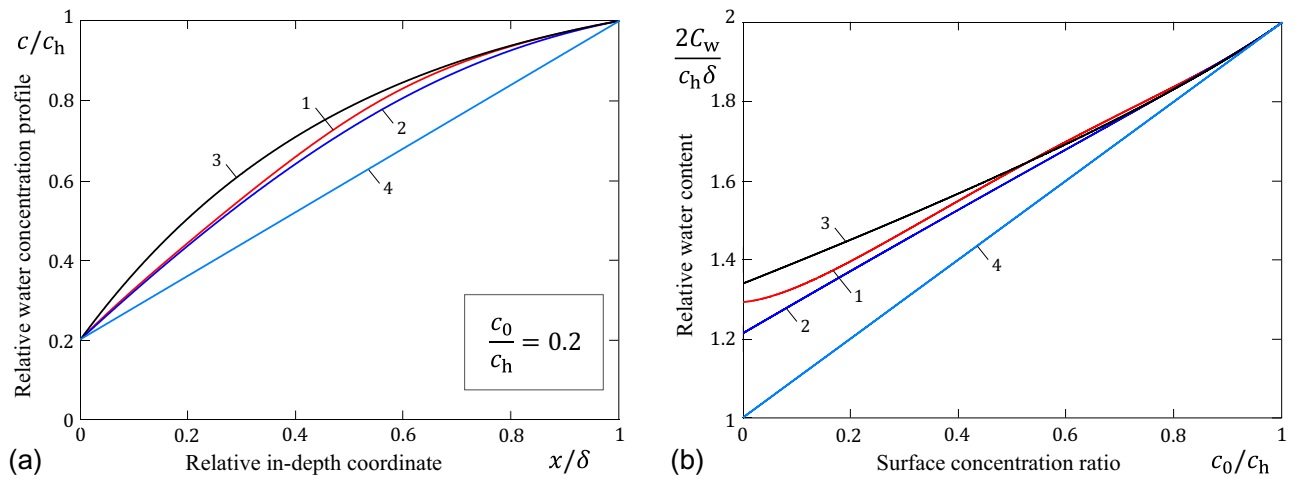


Figure 3. (a) Water concentration profile in stratum corneum; (b) Water content in stratum corneum. Curves 1, 2, and 3 correspond to formulas (1), (2), and (3), respectively. The straight line (curve 4) represents the constant diffusivity model.

the Fujita approximation (3) overestimates the water concentration profile compared to the bi-exponential approximation (1), though the Fujita parameters were determined by the best fitting to formula (1).

Water content. Further, by rearranging the steady-state form of Eq. (4)₂ in the form $c \, dx = (1/J_\infty)cD(c) \, dc$, where the constant J_∞ is given by (6), and integrating over the stratum corneum thickness (when $x \in (0, \delta)$ and $c \in (c_0, c_h)$), we can evaluate the water content

$$C_w = \int_0^\delta c \, dx = \delta \left(\int_{c_0}^{c_h} D(u) \, du \right)^{-1} \int_{c_0}^{c_h} uD(u) \, du, \tag{8}$$

where c under the integral sign in the first formula (8) is regarded as a function of the depth x according to Eq. (7). It is also to note that the water content is proportional to the wet thickness δ of the SC membrane.

The variation of the relative water content $2C_w/c_h\delta$ as a function of the surface concentration ratio c_0/c_h is illustrated in Fig. 3b for typical variations of the SC diffusivity. The dependence on the relative humidity of ambient air enters the right-hand side of formula (8) via the lower integration limit c_0 .

Thickness of stratum corneum. Following¹⁰, we relate the SC thickness to the thickness of the dry SC membrane as

$$\delta_d = \int_0^\delta \left(1 - \frac{c}{\rho_w} \right) dx, \quad \delta = \delta_d \left(\int_{c_0}^{c_h} \left(1 - \frac{u}{\rho_w} \right) D(u) \, du \right)^{-1} \int_{c_0}^{c_h} D(u) \, du, \tag{9}$$

where Eq. (9)₂ is derived from Eq. (9)₁, using Eq. (7).

We note that by the substitution of the second relation (9) into Eq. (8), we can evaluate the water content in the form (see SI, Section V, formula (23)), from where it is readily seen that the in vivo water content of the SC membrane is proportional to the SC dry thickness δ_d and is independent of the absolute value of the diffusivity, since the right-hand side of this expression is invariant with respect to the scaling transformation $D \mapsto \Lambda D$ for any positive constant Λ . However, the value of C_w is sensitive to the form of the functional dependence of the diffusivity D on the water concentration c .

The SC thickness, δ_h , in the fully hydrated state, when $c_0 = c_h$, can be evaluated in the form $\delta_h = \delta_d(1 - c_h/\rho_w)^{-1}$. We note that $\delta < \delta_h$ for any $c_0 < c_h$.

Assessment of the SC water diffusivity from the water concentration profile. By rearranging Eq. (4)₂, we arrive at the following well-known equation⁸:

$$D(c) = J_\infty \frac{dx}{dc}. \tag{10}$$

The equation above allows to evaluate the function $D(c)$ in the interval $c \in (c_0, c_h)$, provided the water concentration profile is measured in vivo.

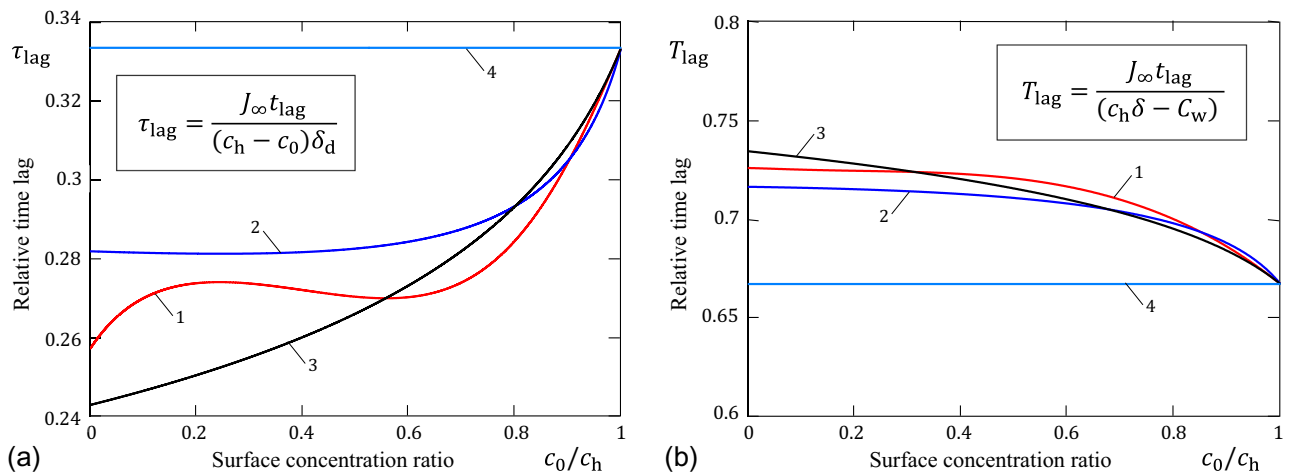


Figure 4. Time lag for stratum corneum relative to the SC dry (a) and wet (b) bases. Curves 1, 2, and 3 correspond to formulas (1), (2), and (3), respectively. The straight line (curve 4) represents the constant diffusivity model.

Time lag associated with desorption after application of occlusion. A so-called POST (plastic occlusion stress test) has been proposed¹³ for measuring the water desorption curve after removal of the occlusion. When a water-impermeable plastic patch is applied to the surface of SC, the steady-state water concentration profile changes to reach a uniform distribution, as shown in Fig. 2b. When the occlusive patch is removed, the dynamic desorption process occurs, during which the water concentration profile gradually returns to the steady-state form. This desorption process is characterized by the skin surface water loss (SSWL), which has the same units as TEWL, but is a function of time.

By the definition, we put

$$J_0(t) = D(c(x, t)) \left. \frac{\partial c(x, t)}{\partial x} \right|_{x=0} \tag{11}$$

The initial condition for the third stage of POST is $c|_{t=0} = c_h, x \in (0, \delta_h)$, where δ_h is the thickness of the fully hydrated SC membrane.

The total water loss (per unit area of the SC free surface) will be given by the integral

$$Q_0(t) = \int_0^t J_0(\tau) d\tau. \tag{12}$$

It can be shown^{14,15} that with increasing time the function $Q_0(t)$ approaches the asymptote $Q_a(t) = J_\infty(t + t_{lag})$, where the time lag t_{lag} is given by the following formula:

$$t_{lag} = \left(\int_{c_0}^{c_h} D(u) du \right)^{-3} \left(\delta^2 \int_{c_0}^{c_h} D(u)(c_h - u) \int_u^{c_h} D(w) dw du \right). \tag{13}$$

The time lag is one of the essential parameters accessible in experiments, and expresses the time it would have taken in steady state to lose the excess water loss during the POST protocol.

To compare the excess water loss $J_\infty t_{lag}$ during the POST protocol to the water available to diffusion, the relative time lags $\tau_{lag} = J_\infty t_{lag} / (c_h - c_0)\delta$ and $T_{lag} = J_\infty t_{lag} / (c_h\delta - C_w)$ are defined, where C_w is the water content in the steady state. Their variations as functions of the surface concentration ratio c_0/c_h are illustrated in Fig. 4 for the typical variations of the SC diffusivity. It is of interest to note that the variation of t_{lag} as a function of c_0 for the bi-exponential approximation (1) is not monotonic.

We also note that, in view of (12), the following important formula holds true:

$$t_{lag} = \int_0^\infty \left(\frac{J_0(t)}{J_\infty} - 1 \right) dt. \tag{14}$$

While Eq. (13) allows for the analytical study of the desorption time lag, formula (14) is very useful in the analysis of experimental data. Finally, we note that the value of t_{lag} , as it is readily seen from (13), is positive.

It is interesting to note¹⁵ that for the diffusion coefficient $D(c)$ being a strictly-increasing function of the concentration c , the desorption time lag is less than the adsorption time lag. This theoretical fact agrees with the simulation results¹⁶ showing that desorption rates from hydrated SC are faster than hydration rates of dry SC and, apparently, has implications in simulations of the baby diapering scenarios.

Remark 1 It is instructive to write out the solutions in the case of constant diffusivity. So, assuming that $D \equiv \text{const}$, Eqs. (6), (7), (8), (9), and (13) yield

$$c = c_0 + (c_h - c_0) \frac{x}{\delta}, \quad J_\infty = (c_h - c_0) \frac{D}{\delta}, \quad t_{\text{lag}} = \frac{\delta^2}{3D} = \frac{2}{3} \frac{(c_h \delta - C_w)}{J_\infty}, \quad (15)$$

$$C_w = \frac{(c_h + c_0)}{2} \delta, \quad \delta = \left(1 - \frac{(c_h + c_0)}{2\rho_w}\right)^{-1} \delta_d. \quad (16)$$

It is interesting to highlight that in this special case, t_{lag} does not depend on the ratio between c_0 and c_h .

Desorption from a semi-infinite medium. In regard to the analysis of a concentration-dependent desorption after application of occlusion up to the so-called breakthrough time¹⁷, it is of interest to consider the following problem of an semi-infinite interval in contact with a sink. The desorption from a finite medium in the case of constant diffusivity is considered in Supplementary Information (SI) (see Section I).

We have proved (see SI, Section II) that the water flux from a Fujita semi-infinite medium with the initial $c|_{t=0} = c_h$ and boundary $c|_{x=0} = c_0$ conditions is given by

$$J_0(t) = \kappa_1 (c_h - c_0) \sqrt{\frac{D_1}{t}}, \quad t > 0, \quad (17)$$

where we have introduced the shorthand notation

$$\kappa_1 = \frac{1}{\lambda_1} \sqrt{\frac{2(1 - \lambda_1)}{\mu_1}}, \quad D_1 = \frac{D_0}{1 - \lambda c_0}, \quad \lambda_1 = \frac{\lambda(c_h - c_0)}{1 - \lambda c_0}, \quad (18)$$

and the dimensionless parameter μ_1 is defined as the root of the equation

$$\int_0^1 \frac{d\varphi}{\sqrt{\varphi^2 - 2\mu_1 \ln \varphi}} = -\frac{1}{2} \ln(1 - \lambda_1). \quad (19)$$

Interestingly, the inverse square root time variation obtained for the water loss (17) is a characteristic feature of the general concentration-dependent desorption from a semi-infinite medium.

Finally, we note that the dimensionless parameter κ_1 , which is defined by formula (18)₁, depends on the ratio c_h/c_0 besides the parameter λ that enters the Fujita formula (3).

Reformulating the boundary conditions in terms of relative humidity. In practice, the surface water concentration c_0 cannot be simply controlled in a direct way. Indeed, one can easily control the external relative humidity (RH) and, correspondingly, the surface water activity $a_w^0 = \text{RH}/100\%$.

The relation between the water volume fraction ϕ_w and the water activity a_w is provided by the sorption isotherm $\phi_w = f(a_w)$, which is measured in thermodynamic equilibrium under constant temperature. Thus, if a_w^0 denotes the water activity at the SC surface, then we will have

$$c_0 = \rho_w f(a_w^0). \quad (20)$$

Now, by making use of Eq. (20), we can easily recalculate the TEWL (6) as a function of the external relative humidity, provided the sorption isotherm is known. Finally, we note¹⁸ that the water activity value $a_w^h = 0.996$ can be assumed on the internal side of SC, which corresponds to 99.6% RH.

Results

Main relations of the Fujita approximation-based model. Having presented the basic theoretical relations, we now evaluate the relations for the specific case of the Fujita expression in Eq. (3). By substituting Eq. (3) into Eq. (6)₂, we obtain the dimensionless form of Fujita's relation as

$$\frac{D(c)}{D_0} = \left(1 - \lambda c_h \frac{c}{c_h}\right)^{-1}, \quad (21)$$

The mean diffusion coefficient reads

$$\bar{D} = \frac{D_0}{\lambda(c_h - c_0)} \ln \left(\frac{1 - \lambda c_0}{1 - \lambda c_h}\right), \quad (22)$$

so that, in view of (22), formula (6) for the steady-state water loss TEWL can be rewritten as

$$J_\infty = \frac{D_0}{\lambda \delta} \ln \left(\frac{1 - \lambda c_0}{1 - \lambda c_h}\right). \quad (23)$$

Further, from Eqs. (7) and (8), we arrive at the inverse relation between c and x , which can be solved for water concentration profile $c(x)$ as follows:

$$c = \frac{1}{\lambda} - \left(\frac{1}{\lambda} - c_0 \right) \exp \left\{ -\frac{\lambda J_\infty}{D_0} x \right\}. \quad (24)$$

It is interesting to stress that the water profile is a simple exponential profile, with a spatial decay constant $\lambda J_\infty/D_0$, which, in view of (23), has only one free parameter λ besides the geometrical boundary conditions specifying δ , c_0 and c_h .

The variation of the relative water concentration profile $c(x)/c_h$ as a function of the relative in-depth coordinate x/δ is illustrated in SI (see Section V, Fig. 6a) for the typical surface concentration ratio $c_0/c_h = 0.2$. As expected, a small λ recovers the constant diffusion result, while a larger λ induces a stronger loss of water concentration closer to the surface.

The substitution of Eq. (24) into Eq. (8) yields the water content

$$C_w = \frac{\delta}{\lambda} + \left(\frac{1}{\lambda} - c_0 \right) \frac{D_0}{\lambda J_\infty} \left[\exp \left\{ -\frac{\lambda J_\infty}{D_0} \delta \right\} - 1 \right]. \quad (25)$$

The variation of the relative water content $2C_w/c_h\delta$ as a function of the surface concentration ratio c_0/c_h is illustrated in SI (see Section V, Fig. 6b) for the typical surface concentration ratio $c_0/c_h = 0.2$. We remark that even for low humidity, i.e. low c_0 , a higher λ implies that a significant amount of water is retained in the SC compared to the constant diffusivity model.

Now, the substitution of the Fujita expression (3) for the diffusivity into Eq. (9) yields the relative SC thickness

$$\frac{\delta}{\delta_d} = \left(\frac{c_h - c_0}{\rho_w} + \left(1 - \frac{1}{\lambda \rho_w} \right) \ln \left(\frac{1 - \lambda c_0}{1 - \lambda c_h} \right) \right)^{-1} \ln \left(\frac{1 - \lambda c_0}{1 - \lambda c_h} \right), \quad (26)$$

where δ_d is the SC thickness in the dry state.

From Eqs. (3) and (13), it follows that

$$t_{\text{lag}} = \frac{\lambda \delta}{J_\infty} \left(\ln \frac{1 - \lambda c_0}{1 - \lambda c_h} \right)^{-2} \int_{c_0}^{c_h} \frac{(c_h - u)}{1 - \lambda u} \ln \left(\frac{1 - \lambda u}{1 - \lambda c_h} \right) du. \quad (27)$$

We note that t_{lag} depends on D_0 via J_∞ .

The variation of the relative time lag $\tau_{\text{lag}} = J_\infty t_{\text{lag}}/(c_h - c_0)\delta$ given by formula (27) as a function of the surface concentration ratio c_0/c_h is illustrated in SI (see Section V, Fig. 7a) for the typical surface concentration ratio $c_0/c_h = 0.2$. Fig. 7b (see Section V, SI) illustrates the variation of the relative time lag τ_{lag} as a function of the concentration-dependence parameter λ for various values of the ratio c_0/c_h . Again, the larger the dependence of the diffusivity on the concentration, i.e., the larger λ , the shorter the lag time, as more water is retained compared to the constant diffusivity model for $\lambda = 0$.

Finally, by making use of Eq. (26), we can rewrite formula (23) in the form

$$J_\infty = \frac{D_0}{\lambda \delta_d} \left(\frac{c_h - c_0}{\rho_w} + \left(1 - \frac{1}{\lambda \rho_w} \right) \ln \left(\frac{1 - \lambda c_0}{1 - \lambda c_h} \right) \right). \quad (28)$$

Thus, the Fujita approximation-based model contains only three governing parameters, namely, D_0 , λ , and δ_d . The limiting case $\lambda \rightarrow 0$ corresponds to the constant diffusivity.

Cross-validation of the Fujita approximation-based model. To validate the proposed model, we make use of the data set presented by Blank et al.¹⁰ and employ the inverse analysis to recover the diffusivity data from their TEWL predictions. Since the TEWL variation obtained in¹⁰ is given as a function of relative humidity, we need to utilize a sorption isotherm in order to recalculate the TEWL versus the surface water concentration.

It can be shown (see SI, Section III, Fig. 3), the equilibrium sorption data for human stratum corneum¹⁹, which was used in¹⁰, is well fitted by the GAB (Guggenheim–Anderson–de Boer) model

$$c_w = \frac{\rho_w \rho_{\text{SC}} V_w}{\rho_w + \rho_{\text{SC}} V_w}, \quad \frac{V_w}{V_m} = \frac{Cka_w}{(1 - ka_w)(1 - ka_w + Cka_w)} \quad (29)$$

with the following coefficients²⁰: $\rho_{\text{SC}} = 1.3 \text{ g cm}^{-3}$, $C = 4.39$, $k = 0.9901$, and $V_m = 0.0386 \text{ g water/g dry tissue}$.

It ought to be emphasized that in the literature there are many studies (on subjects from different age and gender groups) addressing post-occlusion water diffusion in human stratum corneum, which were recently summarized by Saadatmand et al.²¹ and analysed using a numerical skin swelling model¹⁶ with the biexponential approximation for the SC diffusivity (1) and the GAB sorption isotherm (29). It was concluded that for describing most of the collected SSWL data, in particular, the value of the GAB parameter k must be reduced similar to earlier microcalorimetry studies of human SC²². In this regard it should be highlighted that the sorption isotherm of SC is known to be influenced by its composition, including the lipid content²³, so that the GAB parameter k is expected to be subject-dependent. In the case under consideration, it has been verified (see SI, Section II, Fig. 2) that the GAB sorption isotherm with the adopted parameters was fitted well to the specific experimental data¹⁹, which was used in the diffusion analysis¹⁰.

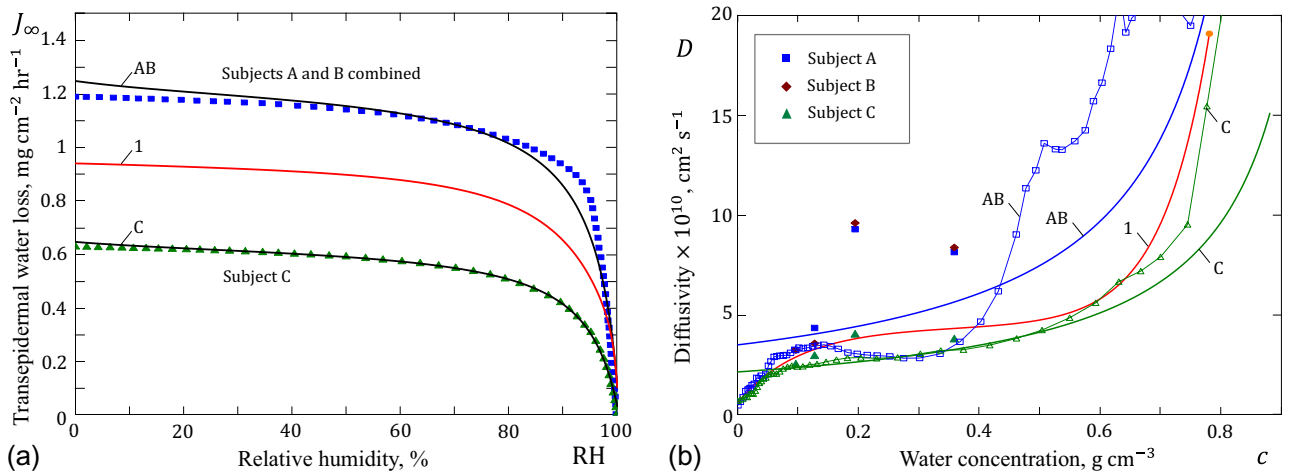


Figure 5. (a) Calculated in vivo steady-state water flux in stratum corneum J_∞ as a function of relative humidity; (b) Water diffusivity of stratum corneum D as a function of water concentration c . The symbolized points are adopted from¹⁰.

It is to emphasize that the TEWL variations (see Fig. 5) were predicted in¹⁰ based on the experimental data for the SC diffusivity (see Fig. 5b) and the equation

$$J_\infty = \frac{1}{\delta_d} \int_{c_0}^{c_h} \left(1 - \frac{u}{\rho_w}\right) D(u) du, \tag{30}$$

which follows from Eqs. (6) and (9).

However, no analytical approximation for the dependence of D on c was reported in¹⁰. Thus, we can regard the TEWL predictions shown in Fig. 5a as our input data for fitting by Eq. (28). Following¹⁰, we assume that $c_h = 0.88 \text{ g cm}^{-3}$ and take $\delta_d = 10 \text{ }\mu\text{m}$ for the SC dry thickness for all subjects (A, B, and C), which experimentally varied from $6 \text{ }\mu\text{m}$ to $13 \text{ }\mu\text{m}$.

So, by fitting the TEWL variations with Eq. (28), we obtain $D_0 = 3.451 \times 10^{-10} \text{ cm}^2 \text{ s}^{-1}$, $\lambda = 1.073 \text{ cm}^3 \text{ g}^{-1}$ for subjects A and B, and $D_0 = 2.092 \times 10^{-10} \text{ cm}^2 \text{ s}^{-1}$, $\lambda = 0.979 \text{ cm}^3 \text{ g}^{-1}$ for subject C. The corresponding curves for the diffusivity D are shown in Fig. 5b, where the bi-exponential approximation (1) has been shown as well.

On the other hand, the discrete TEWL variations from Fig. 5a can be used directly to evaluate the SC variable diffusivity coefficients of subjects A, B, and C. In this way, from Eq. (30), it follows that

$$D = -\delta_d \left(1 - \frac{c}{\rho_w}\right)^{-1} \frac{dJ_\infty}{dc}. \tag{31}$$

Formula (31) allows us to evaluate the diffusivity D as a function of the water concentration c . It can be used when the TEWL variation $J_\infty(c_0)$ is given in terms of the water concentration c_0 at the free surface of the SC membrane.

Further, by utilizing the general sorption isotherm (20), we can transform Eq. (31) as follows:

$$D = -\frac{\delta_d}{\rho_w(1-f(a_w))} \left(\frac{df(a_w)}{da_w}\right)^{-1} \frac{dJ_\infty}{da_w}. \tag{32}$$

Formula (32) is recommended for the use when the TEWL variation $J_\infty(a_w^0)$ is known in terms of the water activity a_w^0 at the SC surface.

The results of the application of Eq. (32) to the discrete TEWL variations shown in Fig. 5a, when the sorption isotherm is described by the GAB model (29) are presented in Fig. 5b. It is of interest to observe that, in contrast to the Fujita approximation (3), the obtained variations of the SC diffusivity exhibit the decreasing trend as the water concentration decreases. However, this feature is captured by the bi-exponential approximation (1). It is to note that the scattering of the diffusivity discrete variations observed in Fig. 5b can be partially explained by the digitalization errors as well as by the numerical errors due to the graphical differentiation employed.

It should be noted that the developed model assumes the Dirichlet-type boundary conditions (5) on both sides of the SC membrane. However, when the surface of skin is exposed to moving air, it is known^{16,21} that the Robin-type boundary condition, which relates the water flux at the skin surface to the difference ($a_w^0 - \text{RH}/100$) with a mass transfer coefficient being dependent on the indoor wind velocity, would be more realistic. In this case, in view of Eq. (20), the water activity at the SC outer surface can be evaluated as $a_w^0 = f^{-1}(c_0/\rho_w)$, where $f^{-1}(\phi_w)$ is the inverted sorption isotherm. Correspondingly, the boundary condition at the skin surface will be non-linear and numerical methods will be needed even for solving the steady-state diffusion problem with account for a discontinuity between water activity at the skin surface a_w^0 and that in the surrounding air, which is

given by $RH/100$. This effect manifests itself in comparison of Curve 1 from Fig. 5a with the calculated water flux (TEWL) through SC obtained by Li et al.¹⁶ (see their Fig. 3, where the dry SC thickness is taken to be $9.55 \mu\text{m}$). To the best of the authors' knowledge, there are no published studies on a parametric analysis of this problem that addresses the effect of the boundary layer resistance on TEWL.

Interpretation of the Fujita parameters. First of all, we observe that both Fujita parameters D_0 and λ that enter formula (3) are dimensional. In the case of stratum corneum, when the water concentration inside the SC membrane varies between the boundary values c_0 and c_h , it makes sense to represent the Fujita approximation (3) in the form

$$D = D_0 \left(1 - \bar{\lambda} \frac{c}{c_h} \right)^{-1}, \quad \bar{\lambda} = \lambda c_h. \quad (33)$$

The relative diffusivity curve D/D_0 is shown in Fig. 8a (see Section V, SI) in the logarithmic scale for different values of the concentration-dependence parameter $\bar{\lambda}$. Figure 8b (see Section V, SI) illustrates the variation of the relative diffusivity $D(c_0)/D_0$ in the logarithmic scale as a function of the concentration-dependence parameter $\bar{\lambda}$ for various values of the ratio c_0/c_h . Larger values of λ and $\bar{\lambda}$ induce a larger sensitivity of the diffusion coefficient on the local concentration. As a more practical interpretation, λ represents the slope of D in the limit of $c = 0$, and in addition induces more spread of the diffusivities at larger c . We remark that λ has to be chosen smaller than $1/c_h$, i.e. $\bar{\lambda} < 1$, to avoid an unphysical divergence of the diffusion coefficient.

We note that in the example considered in section “Cross-validation of the Fujita approximation-based model”, we have $\bar{\lambda} = 0.944$ for subjects A and B, and $\bar{\lambda} = 0.862$ for subject C.

Further, the Fujita parameter D_0 has a simple interpretation as the diffusivity at zero concentration, that is $D_0 = D(0)$. However, as it was already pointed out before, the Fujita approximation in Eq. (33)₁ does not describe the variation of the diffusivity for dry SC, and therefore, the value of D_0 should not be accepted as characteristic for keratinous tissues⁹.

The diffusivity of SC in the fully hydrated state, which according to Eq. (33)₁ is predicted to be $D_h = D_0/(1 - \bar{\lambda})$, should also be considered with care for characterization of permeabilities of different SC membranes, as the value of D_h is difficult to measure experimentally²⁴.

By taking into account the fact that TEWL measurements allow to easily estimate the mean diffusivity, it seems logical to characterize different SC membranes by the mean diffusivity coefficient \bar{D} defined by formula (6)₂ for comparison. However, a complication appears when TEWL tests are performed at different levels of air humidity, as the mean diffusivity \bar{D} depends on the water concentration c_0 at the free surface. In this case, one can introduce a standard relative humidity RH_s and, correspondingly, according to the sorption isotherm (20), a standard water concentration at the SC surface as

$$c_s = \rho_w f \left(\frac{RH_s}{100} \right). \quad (34)$$

Then, in view of (33)₂, formula (22) yields the Fujita mean diffusivity at standard air humidity

$$\bar{D}_s = \frac{D_0}{\bar{\lambda}(1 - c_s/c_h)} \ln \left(\frac{1 - \bar{\lambda}c_s/c_h}{1 - \bar{\lambda}} \right), \quad (35)$$

where c_s is fixed according to Eq. (34).

Thus, in the framework of the Fujita approximation (33), the diffusivity properties of SC can be comparatively characterized by the dimensionless concentration-dependence parameter λ and the mean diffusivity \bar{D}_s , defined by formula (35) for a certain standard level of ambient humidity.

Analysis of post-occlusion skin surface water loss. From Eq. (17), it follows that the SSWL in some initial time interval $(0, t_1)$ after the occlusion removal varies in such a way that

$$\sqrt{t} J_0(t) \simeq \kappa_1 (c_h - c_0) \sqrt{D_1}, \quad t \in (0, t_1). \quad (36)$$

In view of (18) and (33)₂, we have

$$D_0 = D_1 \left(1 - \bar{\lambda} \frac{c_0}{c_h} \right), \quad \lambda_1 = \frac{\bar{\lambda}(1 - c_0/c_h)}{1 - \bar{\lambda}c_0/c_h}. \quad (37)$$

The dimensionless factor κ_1 that enters the right-hand side of relation (36) depends on both the ratio c_0/c_h of the water concentrations at the boundaries and the dimensionless Fujita concentration-dependence parameter $\bar{\lambda}$ via the variable λ_1 (see Eq. (37)₂). It can be easily verified that $\lambda_1 \in (0, 1)$, provided that $c_0 < c_h$ and $\bar{\lambda} \in (0, 1)$. While the physical interpretation is challenging, λ_1 represents a universal variable, from which realistic values of λ can be obtained via rescaling. The variation of the SSWL factor κ_1 versus λ_1 is shown in SI (see Fig. 2b). We note that $\kappa_1(0) = 1/\sqrt{\pi} = 0.564 \dots$ Observe that the derivative $d\kappa_1/d\lambda_1$ tends to infinity as λ_1 tends to 1. This means that for the values of $\bar{\lambda}$ close to 1, a small error in the determination of $\bar{\lambda}$ will lead to a larger error in the evaluation of κ_1 .

Further, we note that as the time variable t increases, the SSWL $J_0(t)$ tends to its limit value J_∞ that determines the TEWL. In view of Eq. (33)₂, Eq. (23) can be represented as

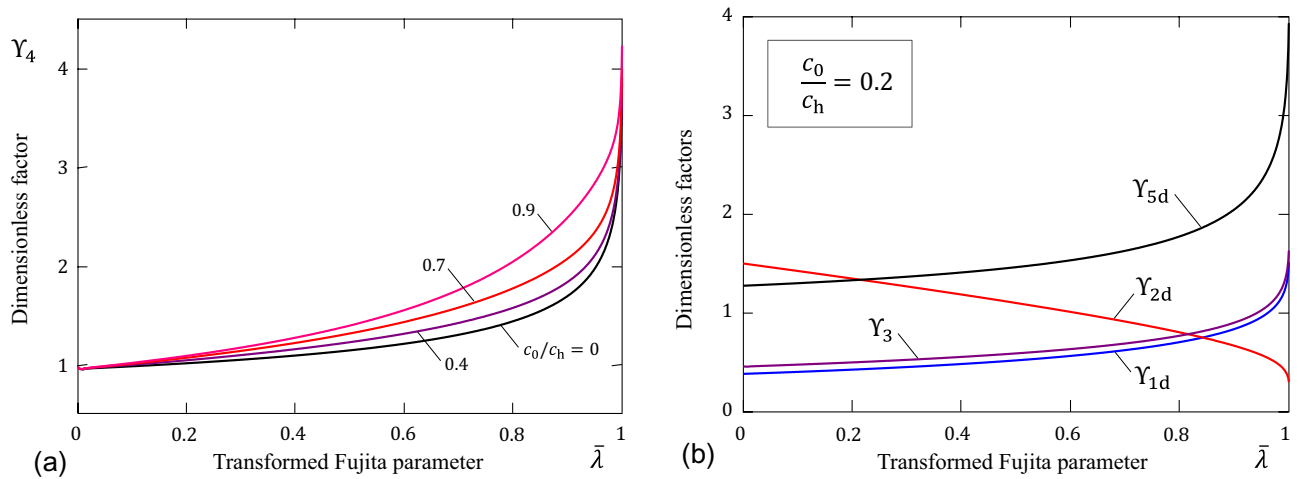


Figure 6. (a) Variation of the right-hand side of Eq. (42); (b) Variation of the dimensionless factors.

$$J_{\infty} = \frac{D_0 c_h}{\delta} \Upsilon_1. \tag{38}$$

The variation of the TEWL factor Υ_1 is shown in SI (see Fig. 4, Section IV).

Finally, by taking into account Eqs. (13) and (33), the time lag can be represented as

$$t_{lag} = \frac{\delta^2}{D_0} \Upsilon_2. \tag{39}$$

The variation of the time lag factor Υ_2 is shown in SI (see Fig. 5, Section IV).

Observe that, generally speaking, formulas (36)–(39) contain three unknown parameters D_0 , $\bar{\lambda}$, and δ , since the surface concentration ratio c_0/c_h is assumed to be specified. For their determination, we have got two equations (38) and (39), and yet one approximate relation, which can be obtained by fitting the approximate formula (36) to the initial SSWL data.

Let us introduce the so-called SSWL intensity factor, K_0 , as the coefficient of the square-root singularity in the asymptotic approximation

$$J_0(t) \simeq \frac{K_0}{\sqrt{t}}, \quad t \rightarrow 0. \tag{40}$$

Then, in view of (36), (37), and (40), the approximate relation mentioned above can be written in the form

$$K_0 = c_h \sqrt{D_0} \Upsilon_3. \tag{41}$$

The dimensionless factor Υ_3 is given in SI (see formula (18), Section IV) and illustrated in Fig. 6b.

Thus, three equations (38)₁, (39)₁, and (41)₁ can be solved for D_0 , $\bar{\lambda}$, and δ . With this aim, by making use of Eq. (38) and (39), we obtain the relation $D_0 = J_{\infty}^2 t_{lag} c_h^{-2} \Upsilon_1^{-2} \Upsilon_2^{-1}$, from where the wet SC thickness δ has been excluded. Then, the substitution of the derived expression for D_0 into Eq. (41) leads to the equation

$$\frac{K_0^2}{J_{\infty}^2 t_{lag}} = \Upsilon_4, \tag{42}$$

where we have introduced the notation $\Upsilon_4 = \Upsilon_1^{-2} \Upsilon_2^{-1} \Upsilon_3^2$.

The variation of Υ_4 as a function of $\bar{\lambda}$ is shown in Fig. 6a. It should be noted that since $\Upsilon_1 \rightarrow 1 - c_0/c_h$ and $\Upsilon_2 \rightarrow 1/3$ as $\bar{\lambda} \rightarrow 0$, we find that $\Upsilon_3 \rightarrow 3/\pi$ as $\bar{\lambda} \rightarrow 0$ for any value of the ratio c_0/c_h .

Modeling the hypotheses of age-related changes in SC diffusivity. Following², we adopt the following consensus that (I) baseline TEWL does not change significantly with increasing age. At the same time, (II) initial values of the POST-induced SSWL were found to be significantly greater in old skin than in young². In other words, the SSWL intensity factor K_0 increases with age. Moreover, it is also known that (III) water content in aged skin is lower than in young⁴, and (IV) no young/old differences were noted in the SC thickness²⁵. Finally, it as observed² (V) relaxation of SSWL, $J_0(t)$, to TEWL, J_{∞} , is expected to be significantly slower in the aged subjects. In other words, the time lag t_{lag} increases with age.

For what follows, it is convenient to represent formulas (26), (38), and (39) in the form

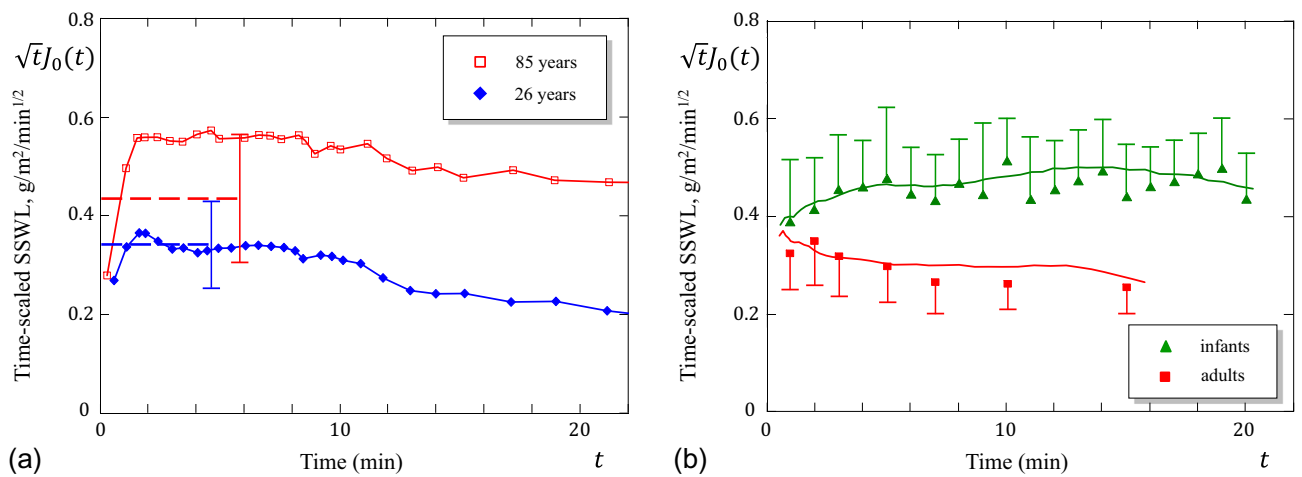


Figure 7. (a) Time-scaled variation of the post-occlusion SSWL based on data from Ref.². The dashed lines correspond to the mean values of $J_{30''}$ obtained from 26 young (19–42 years) and 18 old (69–85 years) subjects. (b) Time-scaled variation of the post-occlusion SSWL based on data from Ref.²⁶.

$$\delta = \delta_d \Upsilon_0, \quad J_\infty = \frac{D_0 c_h}{\delta_d} \Upsilon_{1d}, \quad t_{\text{lag}} = \frac{\delta_d^2}{D_0} \Upsilon_{2d}. \quad (43)$$

For the sake of completeness, we rewrite formula (25) for the water content in two forms (on both a wet and dry basis) as follows:

$$C_w = c_h \delta \Upsilon_5, \quad C_w = c_h \delta_d \Upsilon_{5d}. \quad (44)$$

The dimensionless factors Υ_0 , Υ_{1d} , Υ_{2d} , Υ_5 , and Υ_{5d} are given in SI (Section IV, formulas (19)–(22)).

Based on the experimental data obtained by Roskos and Guy², the ratio of the characteristic time for water diffusion across the SC membrane in the old group to that in the young group is found to be $t_{\text{lag}}^{\text{old}}/t_{\text{lag}}^{\text{young}} = 360/175 \approx 2.06$. In addition, the ratio $K_0^{\text{old}}/K_0^{\text{young}}$ of the SSWL intensity factors can be estimated from the ratio $J_{30''}^{\text{old}}/J_{30''}^{\text{young}} = 37/29 \approx 1.28$ of the SSWL rates at $t = 30$ sec post-occlusion (see Fig. 7a).

Based on the experimental data obtained by Zimmerer et al.²⁶ we have recalculated the time-scaled variation of the SSWL decay curves, representing the mean of 10 determinations for infants and adults after, respectively, one-hour or two-hour wearing of a diaper or a patch of diaper material. A marked difference is observed between infant and adult skin (see Fig. 7b). It remains a question for further research, and beyond the scope of the present article, to resolve at what age do the water handling properties of skin begin to change.

Therefore, under assumption (I) the quantity $K_0^2/J_\infty^2 t_{\text{lag}}$ on the left-hand side of Eq. (42) markedly decreases with age. Thus, since the quantity Υ_4 on the right-hand side of Eq. (42) depends only on one diffusion parameter, we conclude that, in the framework of the developed model (see Fig. 6), the dimensionless Fujita concentration-dependence parameter $\bar{\lambda}$ should decrease with age.

To verify this hypothesis, we consider the variation of the water content with age, as it follows from Eqs. (44), this quantity is essentially independent of the dimensional diffusivity parameter D_0 . From Fig. 6b, it is seen that the water content factor on dry basis Υ_{5d} decreases with decreasing $\bar{\lambda}$, which is in agreement with assumption (III) under assumption (IV).

Further, according to assumption (V), the time lag t_{lag} increases with age, and this trend is mirrored in the variation of the time lag factor on dry basis Υ_{2d} when the Fujita parameter $\bar{\lambda}$ decreases (see Fig. 6b).

Finally, the effect of the diffusivity parameter D_0 manifests itself in both SSWL and TEWL (see Eqs. (40), (41), and (43)). We observe that according to assumption (II) the SSWL intensity factor K_0 increases with age by about 30%², whereas the effect of decreasing $\bar{\lambda}$ on K_0 is opposite (see the variation of the SSWL factor Υ_3 in Fig. 6b). Hence, the SC diffusivity parameter D_0 should increase with age. When regarding assumption (I), the effect of increasing D_0 on TEWL is compensated by the TEWL factor on dry basis Υ_{1d} , which should decrease with age (see Fig. 6b).

Discussion and conclusions

Let us recall that the developed model contains a number of parameters, namely, the two Fujita diffusivity constants D_0 and $\bar{\lambda}$, the dry SC thickness δ_d , and the water concentration c_h of fully hydrated SC. In addition, the water concentration at the free surface c_0 is a controlling parameter, which varies in response to the change of the water activity at the SC free surface a_w^0 according to the sorption isotherm (20), whose functional dependence may depend on a couple of fitting constants (see, e.g., the GAB model (29)).

In our numerical analysis, we assumed that $c_h = 0.88^{10}$, but there would be only small changes in Fig. 6, if one takes $c_h = 0.78^7$. The effect of the sorption isotherm variation²⁷ will be seen in the dependence of TEWL as a function of the external relative humidity (see Fig. 5). Therefore, if experimental data for TEWL are reported

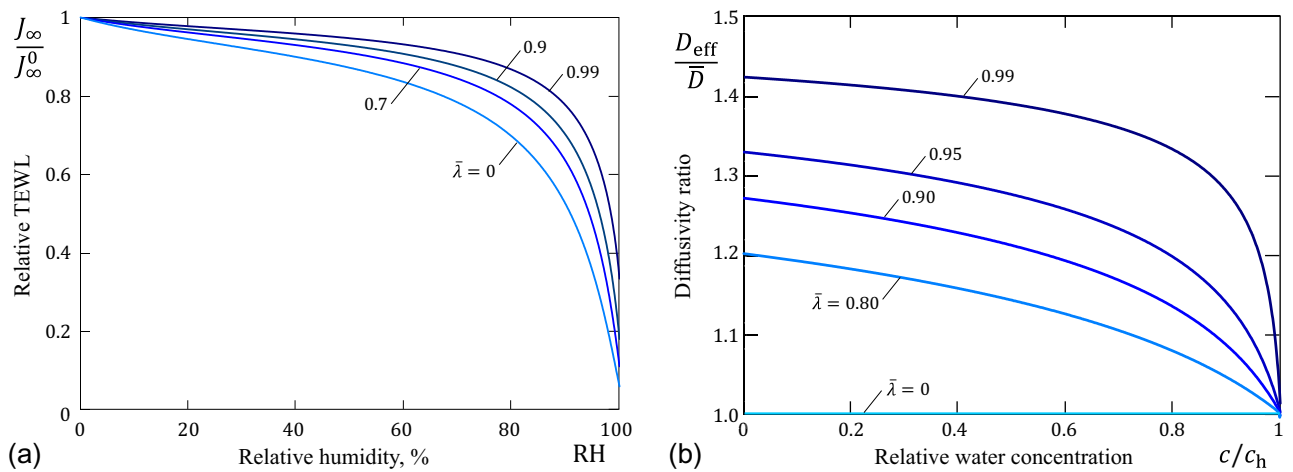


Figure 8. (a) Variation of the ratio of the transepidermal water flux J_∞ to the maximum value $J_\infty^0 = J_\infty|_{a_w=0}$ versus the environmental RH; (b) Ratio of the effective diffusivity D_{eff} to the mean diffusivity \bar{D} .

in terms of relative humidity, then for correct evaluation of the SC diffusivity versus the water concentration, the corresponding sorption isotherm should be reported as well.

As it was previously observed¹⁰, the transepidermal water flux keeps a nearly constant value as the environmental RH varies from 0% to 80%. It is of interest to consider the effect of the dimensionless Fujita diffusivity parameter $\bar{\lambda}$ on the variation of TEWL. Fig. 8a shows that the ability of SC to maintain the TEWL that does not vary much in this range of RH slightly depends on the value of $\bar{\lambda}$. So, in view of age-related variations of $\bar{\lambda}$, this SC barrier function may be expected to weaken with age. However, it should be noted that the age effect on the sorption isotherm has been neglected, as the relative TEWL curves in Fig. 8a are drawn for the same GAB isotherm (29).

It should be noted that though the GAB isotherm (29) shows good fitting of experimental results (see SI, Section III, Fig. 3), there are difficulties in interpreting the GAB parameters from a thermodynamic point of view²⁰. Moreover, in the context of the present theoretical framework it remains an open question to be addressed in future studies whether the sorption isotherm of stratum corneum changes significantly with age.

It is of interest to compare the mean diffusivity \bar{D} , which is measured in the steady state diffusion experiments, with the so-called effective diffusivity, D_{eff} , which can be measured from the initial POST-induced SSWL, provided the data is analyzed using the constant diffusivity model (i.e., by fitting the initial part of the relative post-occlusion SSWL $J_0(t)/(c_h - c_0)$ to the asymptotic approximation $\sqrt{D_{\text{eff}}/\pi t}$). It is to emphasize that the mean diffusivity \bar{D} is determined by formula (6)₂ that also follows from the constant diffusivity model. Thus, if the membrane diffusivity follows the Fujita model (3), then, in view of (17), we have $D_{\text{eff}} = \pi \kappa_1^2 D_1$, where κ_1 and D_1 are given by Eqs. (18)₁ and (18)₂, respectively. The variation of the ratio of D_{eff} to \bar{D} , which is given by Eq. (22), is shown in Fig. 8b, from where it is seen that the difference between the steady-state and dynamic methods for assessing the concentration-dependent diffusivity may be significant.

Finally, let us discuss some possible ways of generalization of the model that can be dealt with analytical mathematical tools. In particular, following Sütterlin et al.²⁸, the flow of calcium, by directed transport coupled to the water flow, can be introduced into the one-dimensional model. On the other hand, there is experimental evidence that the SC membrane hydrates in a non-uniform manner²⁹. However, to account for the effect of the SC morphology, one needs to apply at least a two-dimensional brick-and-mortar geometry modeling framework⁶.

To conclude, the developed mathematical modeling framework has a high potential for analyzing the effect of the dependence of the SC diffusivity on the water concentration, which may change in response to a number of factors, including age-related physiologic changes. We remark that the developed solution of the Fujita model is not only relevant for the biological SC, but can as well be used to describe and predict diffusivities in synthetic membranes with similar overall functionality of water diffusion on local concentration.

Data availability

The datasets used and/or analysed during the current study available from the corresponding author on reasonable request.

Received: 12 July 2022; Accepted: 17 October 2022

Published online: 26 October 2022

References

- Rodrigues, L. M., Pinto, P. C. & Pereira, L. M. Quantitative description of human skin water dynamics by a disposition-decomposition analysis (DDA) of trans-epidermal water loss and epidermal capacitance. *Skin Res. Technol.* **9**, 24–30 (2003).

2. Roskos, K. V. & Guy, R. H. Assessment of skin barrier function using transepidermal water loss: Effect of age. *Pharm. Res.* **6**, 949–953 (1989).
3. Pinto, P. C. & Rodrigues, L. M. Influence of the time of occlusion on the quantitative parameters obtained by modelling trans-epidermal water loss curves to describe the human cutaneous barrier function in vivo. *Med. Biol. Eng. Comput.* **43**, 771–775 (2005).
4. Potts, R. O., Buras, E. M. Jr. & Chrisman, D. A. Jr. Changes with age in the moisture content of human skin. *J. Investig. Dermatol.* **82**, 97–100 (1984).
5. Fujita, H. The exact pattern of a concentration-dependent diffusion in a semi-infinite medium, part I. *Text. Res. J.* **22**, 757–760 (1952).
6. Mitragotri, S. *et al.* Mathematical models of skin permeability: An overview. *Int. J. Pharm.* **418**, 115–129 (2011).
7. Li, X., Johnson, R. & Kasting, G. B. On the variation of water diffusion coefficient in stratum corneum with water content. *J. Pharm. Sci.* **105**, 1141–1147 (2016).
8. Stockdale, M. Water diffusion coefficients versus water activity in stratum corneum: A correlation and its implications. *J. Soc. Cosmet. Chem.* **29**, 625–639 (1978).
9. El-Shimi, A. F. & Princen, H. Diffusion characteristics of water vapor in some keratins. *Colloid Polym. Sci.* **256**, 209–217 (1978).
10. Blank, I. H., Moloney, J. III., Emslie, A. G., Simon, I. & Apt, C. The diffusion of water across the stratum corneum as a function of its water content. *J. Investig. Dermatol.* **82**, 188–194 (1984).
11. Van Logtestijn, M. D., Domínguez-Hüttinger, E., Stamatas, G. N. & Tanaka, R. J. Resistance to water diffusion in the stratum corneum is depth-dependent. *PLoS One* **10**, e0117292 (2015).
12. Crank, J. *The Mathematics of Diffusion* (Oxford University Press, 1979).
13. Berardesca, E., Herbst, R. & Maibach, H. Plastic occlusion stress test as a model to investigate the effects of skin delipidization on the stratum corneum water holding capacity in vivo. *Dermatology* **187**, 91–94 (1993).
14. Frisch, H. L. The time lag in diffusion. *J. Phys. Chem.* **61**, 93–95 (1957).
15. Ash, R. & Espenhahn, S. E. Transport through a slab membrane governed by a concentration-dependent diffusion coefficient. Part I. The four time-lags: Some general considerations. *J. Membr. Sci.* **154**, 105–119 (1999).
16. Li, X. *et al.* Dynamics of water transport and swelling in human stratum corneum. *Chem. Eng. Sci.* **138**, 164–172 (2015).
17. Ruthven, D. M. Transient behavior of a zeolite membrane under non-linear conditions. *Chem. Eng. Sci.* **62**, 5745–5752 (2007).
18. Sparr, E. *et al.* Controlling the hydration of the skin through the application of occluding barrier creams. *J. R. Soc. Interface* **10**, 20120788 (2013).
19. Spencer, T. S., Linamen, C. E., Akers, W. A. & Jones, H. E. Temperature dependence of water content of stratum corneum. *Br. J. Dermatol.* **93**, 159–164 (1975).
20. Yadav, S., Thiel, S. W., Kasting, G. B. & Pinto, N. G. Thermodynamics of water interactions with human stratum corneum II: Interpretation via the Guggenheim–Anderson–deBoer isotherm. *Chem. Eng. Sci.* **64**, 1480–1487 (2009).
21. Saadatmand, M. *et al.* Skin hydration analysis by experiment and computer simulations and its implications for diapered skin. *Skin Res. Technol.* **23**, 500–513 (2017).
22. Yadav, S., Pinto, N. G. & Kasting, G. B. Thermodynamics of water interaction with human stratum corneum I: Measurement by isothermal calorimetry. *J. Pharm. Sci.* **96**, 1585–1597 (2007).
23. Argatov, I., Engblom, J. & Kocherbitov, V. Modeling of composite sorption isotherm for stratum corneum. *Biochim. Biophys. Acta (BBA) Biomembr.* **1864**, 183910 (2022).
24. Pieper, J. *et al.* Water diffusion in fully hydrated porcine stratum corneum. *Chem. Phys.* **292**, 465–476 (2003).
25. Lavker, R. M. Structural alterations in exposed and unexposed aged skin. *J. Investig. Dermatol.* **73**, 59–66 (1979).
26. Zimmerer, R. E., Lawson, K. D. & Calvert, C. J. The effects of wearing diapers on skin. *Pediatr. Dermatol.* **3**, 95–101 (1986).
27. Silva, C. L. *et al.* Stratum corneum hydration: Phase transformations and mobility in stratum corneum, extracted lipids and isolated corneocytes. *Biochim. Biophys. Acta (BBA)* **1768**, 2647–2659 (2007).
28. Sütterlin, T., Tsingos, E., Bensaci, J., Stamatas, G. N. & Grabe, N. A 3D self-organizing multicellular epidermis model of barrier formation and hydration with realistic cell morphology based on EPISIM. *Sci. Rep.* **7**, 1–11 (2017).
29. Bouwstra, J. A. *et al.* Water distribution and related morphology in human stratum corneum at different hydration levels. *J. Investig. Dermatol.* **120**, 750–758 (2003).

Acknowledgements

This research was carried out in the Biobarriers profile and was funded by the Knowledge foundation (KK-stiftelsen). The authors thank Prof. Johan Engblom for fruitful discussions. The authors also would like to express their sincere gratitude to the Referees for their thoughtful comments and insights into this study.

Author contributions

V.K. conceptualized the research design. I.A. and F.R.-R. worked on model derivation and drafted the manuscript. V.K. edited the paper. All authors discussed the results and reviewed the manuscript.

Funding

Open access funding provided by Malmö University.

Competing interests

The authors declare no competing interests.

Additional information

Supplementary Information The online version contains supplementary material available at <https://doi.org/10.1038/s41598-022-22529-x>.

Correspondence and requests for materials should be addressed to V.K.

Reprints and permissions information is available at www.nature.com/reprints.

Publisher's note Springer Nature remains neutral with regard to jurisdictional claims in published maps and institutional affiliations.



Open Access This article is licensed under a Creative Commons Attribution 4.0 International License, which permits use, sharing, adaptation, distribution and reproduction in any medium or format, as long as you give appropriate credit to the original author(s) and the source, provide a link to the Creative Commons licence, and indicate if changes were made. The images or other third party material in this article are included in the article's Creative Commons licence, unless indicated otherwise in a credit line to the material. If material is not included in the article's Creative Commons licence and your intended use is not permitted by statutory regulation or exceeds the permitted use, you will need to obtain permission directly from the copyright holder. To view a copy of this licence, visit <http://creativecommons.org/licenses/by/4.0/>.

© The Author(s) 2022